JOURNAL OF CATALYSIS **179,** 375–389 (1998)
ARTICLE NO. CA982242

Photothermal Heterogeneous Oxidation of Ethanol over Pt/TiO_2

James C. Kennedy III and Abhaya K. Datye[1]

Center for Microengineered Materials and Department of Chemical & Nuclear Engineering, University of New Mexico, Albuquerque, New Mexico, 87131

Received December 8, 1997; revised July 27, 1998; accepted July 28, 1998

Photothermal catalytic oxidation of ethanol over TiO_2 and Pt/TiO_2 has been investigated. Platinum was deposited on the titania using both photoreduction and adsorption of the $PtCl_6^{2-}$ anion. The nominal weight loadings of Pt were less than 1 wt%. Thermal contributions to ethanol oxidation over Pt could be distinguished from photo-contributions to ethanol oxidation over TiO_2 by comparing illuminated and dark reactions under the same conditions. A significant photothermal synergistic effect was seen for Pt/TiO_2 catalysts. The activity for complete oxidation to CO_2 is much greater than the contribution from photo-oxidation over TiO_2 plus thermal oxidation over Pt. Experiments were conducted to investigate the mechanistic nature of the synergistic effect. The synergistic effect was found to be sensitive to preparation conditions, with photoreduced catalysts having higher activities compared to thermally reduced catalysts prepared by adsorption of the $PtCl_6^{2-}$ anion: The differences between the photo and thermally reduced Pt/TiO_2 are attributed to differing extents of etching of the TiO_2 surface by the acidic solution of chloroplatinic acid. An experiment with layered beds of Pt/TiO_2 and TiO_2 showed that adding unetched TiO_2 to etched Pt/TiO_2 could improve CO_2 production. The photothermal synergistic enhancement of CO_2 production appears to be caused primarily by gas phase transport of intermediates between the two catalyst phases in a mixed series-parallel kinetic pathway. Increased levels of acetaldehyde produced by photo-oxidation over TiO_2 can lead to CO_2 production by thermal reaction of the acetaldehyde over Pt.

INTRODUCTION

Heterogeneous photocatalysis over TiO_2 has been the subject of intense study since Fujishima and Honda (1) reported the photocatalytic splitting of water on TiO_2 electrodes. Much of the research has been driven by the potential application of photo-activated ambient temperature oxidation reactions in eliminating toxic organics from liquid or gas phase environments. Photocatalysis requires illumination with photons having energy greater than the band gap of the semiconductor. For TiO_2, photoexcitation across the band gap requires wavelengths less than about 385 nm. Electron–hole pairs created by the absorption of the incident light can recombine or diffuse to the surface, where they are trapped by TiO_2 surface defects or are transferred to adsorbed surface species. The exact nature of the photocatalytic oxidative mechanism is still unknown, although it is generally accepted that the process involves charge trapping by both the photocatalyst and surface adsorbates. Both hydroxyl radicals (2, 3) and surface trapped holes (4) have been implicated by researchers in heterogeneous oxidative events occurring in the liquid phase. Early photocatalytic studies of heterogeneous gas phase systems, however, suggested activated surface adsorbed oxygen as the active species (5, 6). Cunningham *et al.* (7) suggested that hole capture by a surface lattice oxide ion, together with surface-adsorbed oxygen acting as the oxidants explained the photo-oxidation kinetics of 2-propanol over ZnO. Liu *et al.* (8), comparing photo and thermal oxidation of methanol over TiO_2, proposed that H-atom abstraction by O^- was the rate limiting step for both photo and thermal oxidations. UHV studies (9) have also pointed to oxygen species rather than hydroxyl radicals as major participants in photocatalytic oxidations. Wong *et al.* (10), using single crystal rutile TiO_2 (110), have recently shown that hydroxyls are not necessary for the oxidation of methyl chloride but that O_2 is crucial. In addition, oxygen incorporated into oxidation products originates primarily from oxygen rather than hydroxyl groups. These results strongly imply different oxidative mechanisms and photo-oxidative pathways during photocatalysis of gas phase species, compared to their liquid phase counterparts.

In the liquid phase, addition of Pt and other noble metals to TiO_2 has been found to improve photocatalytic efficiencies (11–13) in many oxidation reactions. A Schottky barrier effect at the noble metal/TiO_2 interface, causing electrons to be transported across the interface to the noble metal, has been invoked to explain improved photoefficiencies (14, 15). The improvement has been explained by decreased electron–hole recombination in TiO_2 caused by improved charge carrier separation caused by hole accumulation at the Pt/TiO_2 interface. Alternative explanations have been related to electron trapping in the noble metal. Evidence for electron trapping was shown by a decrease in the steady

[1] Corresponding author. E-mail: datye@unm.edu.

0021-9517/98 $25.00

state (15) and transient photoconductivity (16) of Pt/TiO_2 versus TiO_2. Electron trapping with subsequent reduction reactions at the metal surface can prevent accumulation of excess electrons and lower semiconductor recombination rates (17, 18). Recently, improved oxidation rates under gas phase conditions have been reported in the oxidation of benzene (19) over platinized TiO_2. UHV studies (20) on platinized single crystal TiO_2 (rutile), however, have cast doubt on Schottky barrier/electron trapping mechanisms as the cause for increased photoefficiencies. No improvement in the photo-oxidation of CO to CO_2 in the presence of preadsorbed oxygen was seen at 105 K for Pt/TiO_2 versus TiO_2.

Improved efficiencies of TiO_2 photocatalysts for complete oxidation of volatile organics to CO_2 and H_2O are needed. At high organic concentrations, where conversions are less than 100%, TiO_2 photo-oxidation can result in a mixture of partial oxidation products. Improved photocatalysts are necessary for effective, economic design of chemical reactors that are intended for environmental applications seeking complete oxidation of toxins. Presently, TiO_2 photo-reactor systems can be limited by both low selectivities for complete oxidation and complete absorption of all useful incident ultraviolet light (<385 nm) over a thin layer (1–4 μm) (21, 22) of TiO_2. Higher selectivities for complete oxidation, and with improved energy efficiencies, may allow photocatalysis to compete in areas traditionally reserved to thermal catalysis.

In this paper we present results of gas phase ethanol oxidation over Pt/TiO_2 photocatalysts under photothermal conditions. We investigate the synergistic influence, if any, of Pt supported on TiO_2 and the mechanistic role that Pt plays in increasing complete oxidation efficiencies. Two mechanistic pathways were considered: (1) desorption of photo-oxidized intermediates produced on the TiO_2 surface and re-adsorption on the Pt surface with associated thermal oxidation; and (2) the influence of an electronic effect such as a Schottky barrier at the Pt/TiO_2 interface or electron trapping by the Pt. Our results suggest that the former mechanism may account for the majority of the observed photothermal synergism.

We first examine TiO_2 photo-thermal activity of ethanol oxidation to provide a baseline comparison to Pt/TiO_2. The photo-thermal activity of Pt/TiO_2 prepared by a photoreduction method is then examined under illuminated conditions, where both Pt and TiO_2 are active, and dark conditions, where only Pt is active. The activity of a physical mixture of Pt/TiO_2-SiO_2 is then compared to Pt/TiO_2 to determine whether the presence of a Schottky barrier at the Pt/TiO_2 interface contributes to improvements in complete oxidation observed for Pt/TiO_2. Higher weight loadings of Pt on TiO_2 are examined and found to reduce activity at lower temperatures. We then examine the effect of catalyst preparation by comparing the activity of Pt/TiO_2 prepared by adsorption of $PtCl_6^-$ followed by thermal reduction of Pt. Finally, we investigate the role of gas-phase transport of intermediates between catalyst phases by means of a layered bed experiment. These experiments are outlined below.

METHODS

Since these studies were undertaken with the goal of developing improved photocatalysts, our approach was to compare conversions of ethanol over TiO_2 with Pt/TiO_2 under identical reaction conditions. In particular, we were interested in the conversion efficiency to CO_2. For these studies the catalyst amount was comparable (7 ± 0.5 mg) and the reactor volumetric residence time (26 s) was constant.

Ethanol was chosen as a probe reactant since one of its intermediates, acetaldehyde, is inefficiently oxidized over TiO_2 and has been identified as a key VOC contaminant in indoor air (23). Although we examined much higher concentrations of ethanol (thousands of ppm) compared to those concentrations that might be found in typical indoor air applications (hundreds of ppm), our results may be extrapolated to lower concentrations under circumstances where conversions are comparable. In addition, there is an informative source of literature concerning oxidation of ethanol over TiO_2 (31, 33, 34) and over Pt (47–50). Since photo-oxidation pathways over TiO_2 and thermal oxidation pathways over Pt are similar, they present an ideal system for studying possible synergies afforded by photothermal conditions.

A key element in the experimental approach was to use thin particulate films of TiO_2 (0.25–1 μm) to enable full illumination of the particulate film. Sauer *et al.* (33) have shown that nonilluminated TiO_2 can cause a buildup of strongly adsorbed partial oxidation intermediates that may confound kinetic studies. Hence, in these experiments, weight loadings of the TiO_2 particulate film on a Pyrex glass surface were maintained at $0.094 \text{ mg/cm}^2 \pm 0.005 \text{ mg/cm}^2$ (total TiO_2 in the reactor ≈ 7 mg). In a separate study (28), an absorption coefficient for TiO_2 particulate films was determined from TiO_2 deposited on a glass substrate. The absorption coefficient was determined at the peak emission wavelength of the UV light source (356 nm). This allowed us to ensure that the TiO_2 particulate films were fully illuminated and to determine the fraction of incident light intensity absorbed by the TiO_2.

In these experiments, we determined the activities of Pt/TiO_2 catalysts under both illuminated and dark conditions. Under dark conditions, activity is solely due to the thermal catalytic action of Pt. TiO_2 shows no dark activity over the range of temperatures studied here. In contrast, under illuminated conditions the contributions of both Pt and TiO_2 must be considered. Comparison of the dark activities is a useful tool for characterizing the total available Pt sites on various Pt/TiO_2 catalysts and establishing a baseline

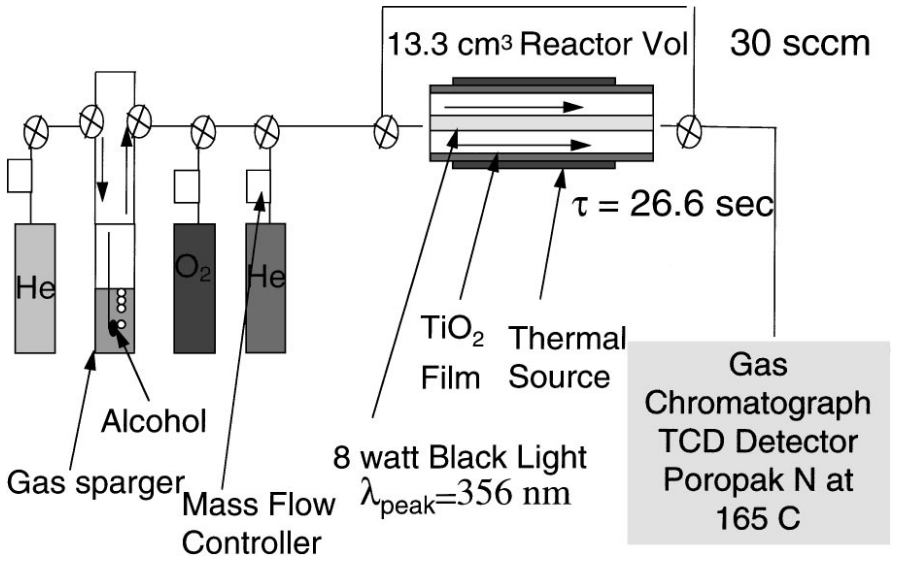

FIG. 1. Gas-phase reactor system used for photocatalytic and thermal studies. The catalyst is coated from an aqueous slurry on the inside radius of the Pyrex tube, while an 8-W UV light source makes up the inside of the annular reactor. The lamp surface is 1 mm from the catalyst particulate film.

with which variations in the illuminated activity can be contrasted.

Photo-Reactor System

Figure 1 shows the annular photo-reactor used in our studies. The photo-reactor has the advantage of allowing a known weight of photocatalyst to be uniformly deposited on the inside of the annulus. Uniform TiO_2 film deposition was accomplished by evenly distributing a TiO_2 slurry inside the Pyrex reactor and evaporating the slurry to dryness while continuously spinning the Pyrex glass tube. The uniformity of deposition could both be seen visually and qualitatively verified by TiO_2 UV absorption measurements of TiO_2 particulate films deposited on Pyrex glass microscopic slides under similar conditions. TiO_2 (Degussa-P25) with a BET surface area of 50 m^2/g was coated from an aqueous slurry on the inside surface of the photo-reactor Pyrex tube. The weighing methodology followed was important to get reproducible and accurate weights. Generally, careful handling procedures (gloved) and long equilibrium times (>1.5 h) were required to allow both the substrate and TiO_2-loaded substrate to reach equilibrium with atmospheric water after being outgassed at about 398 K for 30 min.

The light source was a commercially available 8-W black light (F8 T5/BLB) with a spectral peak at 356 nm. The light flux at the TiO_2 surface was about 2.4×10^{-8} Ein/s-cm^2 (24) by radiometric measurements. The light source inside the tube was the inner diameter of the reactor annulus. The total volume of the reactor was 13.3 cm^3 and the distance between the surface of the light source and the TiO_2 film was 1 mm. Mass flow controllers were used to vary the flow rates of two helium feeds and one oxygen feed. One of the helium feeds was bubbled through the reactant (ethanol) and the second helium feed was used as an inert to vary the relative concentration of the reactant. Changing the relative flow rates of reactant oxygen, and inert gases varied concentrations.

The methodology for experiments at various temperatures consisted of taking a dark measurement followed by an illuminated measurement. After a change in conditions (temperature or illumination), 15 min were sufficient for steady state conditions to be achieved. Kinetic studies, where concentration was varied, were conducted under continuous illuminated or dark conditions. Verification of results was periodically performed by remeasuring results at a given temperature or concentration out of sequence with the normal measuring procedure of sequentially increasing or decreasing temperature. Extended periods (14 h) of continuous photocatalytic operation were conducted where slow deactivation was observed. Deactivation after continuous operation for extended illuminated periods reduced the total conversion by about 7% at concentrations of 6400 ppm ethanol. Studies presented here were conducted over shorter time periods (3 h) and show no significant deactivation.

Heat was applied to the outside of the reactor tube with nylon heating tape, and the temperature determined at the axial midpoint by a thermocouple situated between the heating tape and the outer surface of the Pyrex tube. The reactor tube was heated to temperatures as high as 473 K. The temperature measured on the inside of the reactor tube at the center was within 1 K of the temperature on the outside of the reactor tube. A worst case estimate of the axial temperature profile was determined by measuring temperature on the inside of the reactor tube when open to air.

These measurements revealed an axial temperature profile with the average temperature 80% of the centerline temperature. We report the measured temperature at the reactor tube centerline. Due to the heating effect of the light source, the lowest temperature during reaction was 323 K.

Product Analysis

The reactor effluent was piped directly into a gas-sampling valve connected to a HP 5890 gas chromatograph with a Poropak N column. The column was ramped from 398 K to 448 K during measurement to better separate CO_2 and O_2 peaks. A TCD was used to sample the column effluent and the relative amount of detected species determined by published TCD relative response values (25). It has been shown that, when He is used as a carrier gas, the relative response is independent of detector type and flow rate over a range of carrier gas flow rates (26). Conversion was calculated by taking the product amounts, divided by the reactant, plus product amounts, corrected for stoichiometry. This method reduced errors due to variations in product or reactant condensation on system plumbing. All system plumbing was heated to 373 K to eliminate product or reactant condensation.

One hundred percent conversion gave a stoichiometric amount of products expected for mass balance by GC analysis, according to

$$CH_3CH_2OH + 3\,O_2 \rightarrow 2\,CO_2 + 3\,H_2O. \qquad [1]$$

Titania Photocatalyst

Degussa P25 TiO_2, which has become a standard in photocatalysis research, was used in these studies. P25 has consistently exhibited superior photocatalytic efficiencies when compared to other titanias in liquid-phase photocatalysis research. It is produced by flame hydrolysis of $TiCl_4$ at a temperature greater than 1473 K in the presence of O_2 and H_2. It has been reported (27) as >99.5% pure with residual amounts of SiO_2, Al_2O_3, and trace amounts of Fe_2O_3. Major impurities from elemental analysis are Fe and Ni at <100 ppm. The anatase/rutile ratio is reported (27) as having nominal values of 75% ($\pm$5%) anatase and 25% ($\pm$5%) rutile, a mean specific surface area (BET) of 50 m^2/g, and consists of nonporous primary crystallites in the size range of 20–30 nm. Sedigraph particle size measurements performed on the "as received" powder indicate a mean agglomerate size with an equivalent spherical diameter of about 0.25 μm.

Light Absorptance Characterization

The light absorptance of P25 TiO_2 particulate films was characterized in previous studies (28) by measuring total transmittance and reflectance of the films at various weight loadings of TiO_2. A Cary 14 UV-Vis spectrophotometer equipped with an integrating sphere was used to measure the reflectance and transmittance of TiO_2 particulate films formed on Pyrex slides from an aqueous slurry. Measuring the transmitted and reflected light using an integrating sphere to capture all scattered light is necessary to accurately determine absorption coefficients of particulate films. An absorption coefficient for the P25 TiO_2 particulate films, based on TiO_2 weight loading, was determined to be about 4.2 cm^2/mg. The fraction of the incident light absorbed by a TiO_2 film used in these studies is about 30% according to the Beer–Lambert Law. Our previous studies (28) have also detailed the preparation and morphologies of these particulate films and have shown that P25 TiO_2 films have a well-packed morphology, compared to some other commercially available titanias since they consist of relatively small-sized agglomerates (0.25 μm).

Pt/TiO_2 Photocatalyst Preparation and Characterization

Photoreduced Pt/TiO_2 catalysts were prepared by creating an aqueous slurry of P25 TiO_2, adding an appropriate amount of chloroplatinic acid, $H_2PtCl_6 \cdot 6\,H_2O$, with an equimolar amount of ethanol, and irradiating with a 150-W Hg-Xe lamp for an hour while stirring the solution vigorously (350–500 rpm). The weight loading of TiO_2 in the slurry was about 0.8 wt%. Depending on the amount of chloroplatinic acid added to achieve the desired weight loading, the pH of the solution varied from 3.00 to 2.00. The nominal weight percent of the photoreduced catalysts was estimated by considering the total weight of Pt added. Although atomic absorption spectroscopy showed no remaining Pt in the solution after reaction, it was later determined that some Pt may have deposited on the glass beakers during photodeposition, making the reported weight loadings upper estimates of metal loadings. The resulting Pt/TiO_2 catalysts were either centrifuged or filtered, washed with an equal volume of water, and dried at about 398 K.

Thermally reduced catalysts were prepared by adsorption of the $PtCl_6^{2-}$ ion from chloroplatinic acid. The procedure was the same for the preparation of the photoreduced catalysts except for illumination. In addition, the resulting catalysts were centrifuged and oxidized and reduced at the temperatures indicated in Table 1 for 1 h. Hydrogen chemisorption measurements were made following a procedure of reducing in H_2 at 623 K for 1 h, and then performing chemisorption at 408 K.

HRTEM micrographs were obtained on a 200 kV JEOL 2010 high-resolution electron microscope. Samples were prepared by depositing dry powder on 200 mesh copper grids with holey carbon film.

Table 1 summarizes the Pt/TiO_2 preparation methods and characteristics. The photo-reduced Pt/TiO_2 catalyst, at a nominal Pt weight loading of 0.2 wt%, has Pt particles that are too small to yield adequate contrast in HRTEM images. XPS measurements verified a weight loading of about 0.2 wt% and dark thermal activity confirmed the presence

TABLE 1

Sample Preparation/Characterization

Sample	Pt source	Preparation method	Temp. treatment (air)/(H_2)	Nominal wt% Pt	TEM Pt particle size (nm)	Irrev. H_2 uptake μmoles/g
PD Pt/TiO2 (0.2)	H_2PtCl_6	Photodep	none	0.2	<1	-
PD Pt/TiO2(0.4)	H_2PtCl_6	Photodep	none	0.4	2	2.9
Pcl Pt/TiO2 (0.4)	H_2PtCl_6	Ads	623 K/623 K	0.4	1.3	9.6
Pt/SiO_2	$Pt(NH)_4NO_3$	Ads	573/623 K	0.4	2-10	10.0

of platinum. The pH of the photo-reduction solution was near 3.00. Figure 2a shows the smooth texture of the surface, showing no evidence of acidic etching by the chloroplatinic acid. Figure 2b shows the higher weight loading (0.4 wt%) photo-reduced catalyst. Here, the Pt particles are resolvable and are about 2 nm in diameter. In addition, the surface shows some roughness and the beginning of an amorphous layer from acidic etching of TiO_2. Preparation conditions involved a pH of about 2.00. Chlorine impurities by XPS were about 0.3 at%. Several TiO_2 particles for each of the catalysts of appropriate size and orientation were sampled in an attempt to find highly diffracting conditions that allowed the surface roughness to be examined. The photo-reduced catalyst, PD Pt/TiO_2 (0.4 wt%), has a H_2 uptake that is lower than that expected from TEM particle size measurements and nominal weight loading values. In addition, photo-reduced catalysts exhibited a bluish color, consistent with a stable form of bulk reduced TiO_2. Bulk reduction of TiO_2 has been previously associated with a strong metal support interaction SMSI. Chen *et al.* (29) have reported a reduced, bluish colored TiO_2 after reducing in hydrogen at 1148 K for 6 h. The bluish TiO_2 was not re-oxidized at room temperature but required heating in oxygen at 773 K to recover a white color.

Figure 2c shows a thermally reduced catalyst prepared by adsorption of the $PtCl_6^-$ anion at about pH 2.00. The Pt/TiO_2 catalyst, Pcl Pt/TiO_2 (0.4 wt%) has a roughened surface with an amorphous layer from acidic etching by the chloroplatinic acid. The possibility of the amorphous layer forming from carbon deposition by electron beam interaction with trace hydrocarbons in the vacuum was eliminated. The rate of amorphous carbon deposition was minimal and the micrograph shown in Fig. 2c was taken quickly after moving to a new analysis area. Pt particles are about 1.3 nm in diameter. Oxidation and reduction conditions are shown in Table 1. Hydrogen uptake is about 10 μmol/g catalyst. Chlorine impurities by XPS were about 0.5 at%.

A Pt/SiO_2 catalyst was also prepared by using microspheres of SiO_2 created by the Stöber process (30). BET surface area measurements of the silica were 87 m^2/g which corresponds with an average primary particle size of 33 nm, compared with an average particle size of 30 nm for the Degussa P-25 TiO_2. The Pt $(NH_3)_4^{+2}$ cation was adsorbed onto the silica at pH 8.5. The conditions of oxidation followed by reduction in H_2 are given in Table 1. The irreversible hydrogen uptake was about the same as the Pcl Pt/TiO_2 (0.4 wt%) sample and showed a similar isotherm. Nitrogen impurities were about 0.4 at% by XPS. Figure 2d shows that the Pt is not uniformly dispersed on the silica and shows a range of Pt particle sizes from about 2–10 nm in diameter. Similar hydrogen uptake values of 10 μmol/g catalyst indicates that the number of Pt sites available per gram of catalyst is about the same as the Pcl Pt/TiO_2 (0.4 wt%) sample. For the photocatalytic studies, equal weights of Pt/SiO_2 and TiO_2 were mixed in an aqueous slurry and sonicated to achieve physical mixing. The total weight of the mixture used in the reactor was the same as that in tests on Pt/TiO_2.

RESULTS AND DISCUSSION

Photocatalytic Oxidation of Ethanol over TiO_2

Since it has previously (31) been shown that the application of moderate heat (373 K) can improve the activity of illuminated TiO_2 ($\lambda < 385$ nm) for heterogeneous gas-phase oxidation of alcohols, the investigation of this phenomenon was not a major goal in our research. The results, however, provide a baseline for comparisons to the photoactivity of Pt/TiO_2 catalysts.

Figure 3 shows the photoactivity as a function of temperature for P25 TiO_2. A peak in activity is seen near 373 K. Although not shown, it is important to note that TiO_2 has no dark, or thermal activity for ethanol oxidation over the range of temperatures examined. The total conversion represents the conversion to acetaldehyde plus the conversion to CO_2. Formaldehyde was detected in minor amounts under illuminated conditions, up to a maximum of 1.5% of the total conversion. While acetaldehyde, ethanol, and carbon dioxide were the major detected products, for clarity in presentation we have chosen in most figures to show the total conversion and the conversion to CO_2. The difference between the total conversion and the conversion to CO_2 represents the conversion to acetaldehyde.

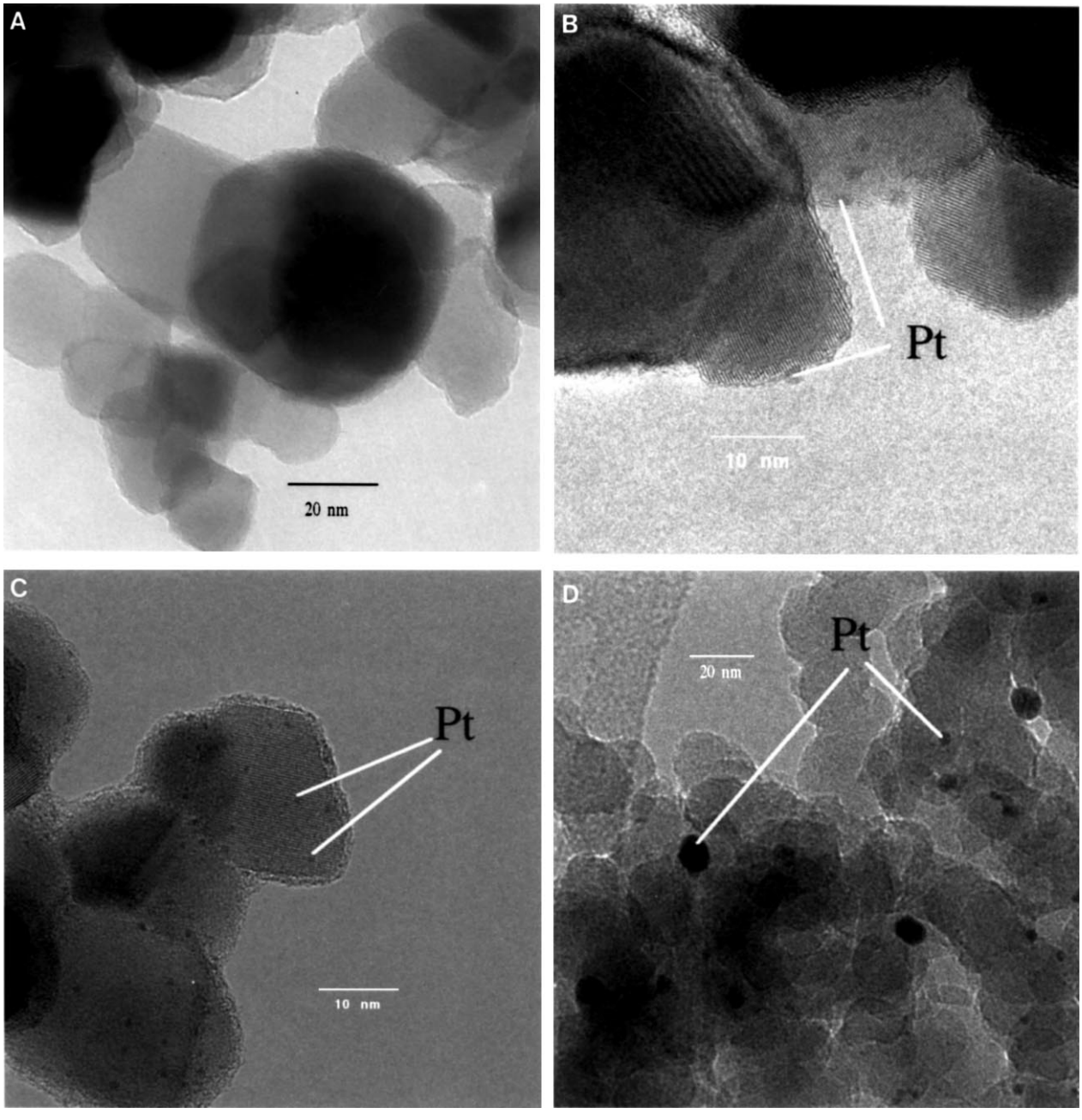

FIG. 2. HRTEM micrographs of (A) photo-reduced Pt/TiO_2 0.2 wt% Pt (PD Pt/TiO_2 0.2 wt%). Pt particles are less than 1 nm in size and not resolvable by HRTEM. The TiO_2 particles have a smooth appearance with no evidence of acidic etching by the chloroplatinic acid. (B) photo-reduced Pt/TiO_2 0.4 wt% Pt (PD Pt/TiO_2 0.4 wt%). There is some evidence of surface roughness caused by acidic etching by chloroplatinic acid at about pH 2.00. (C) Thermally reduced catalyst prepared by adsorption of the $PtCl_6^-$ anion at about pH 2.00, followed by oxidation in air and reduction in H_2 (Table 1). The TiO_2 surface shows extensive acidic etching with the formation of an amorphous layer. (D) Pt supported on SiO_2 nanospheres at 0.4 wt% Pt loading. Pt particle sizes vary from 2–10 nm.

The peak in activity around 373 K was not unexpected since Blake *et al.* (31) saw similar behavior in the oxidation of butanol over TiO_2. These researchers, however, did not suggest an explanation for this effect. It seems likely that adsorption–desorption processes are involved, since these processes are thermally activated, in contrast with photo-activated ethanol oxidation over TiO_2. In addition, both H_2O and ethanol adsorbed on powdered anatase have broad desorption peaks centered at 410 and 380 K, respectively (32). In the work of Muggli *et al.* (34), both water and ethanol were found to be quite strongly bound, with desorption temperatures well in excess of 400 K. However, it should be noted that their TiO_2 samples have been heated at temperatures >773 K. In contrast, all of our experiments

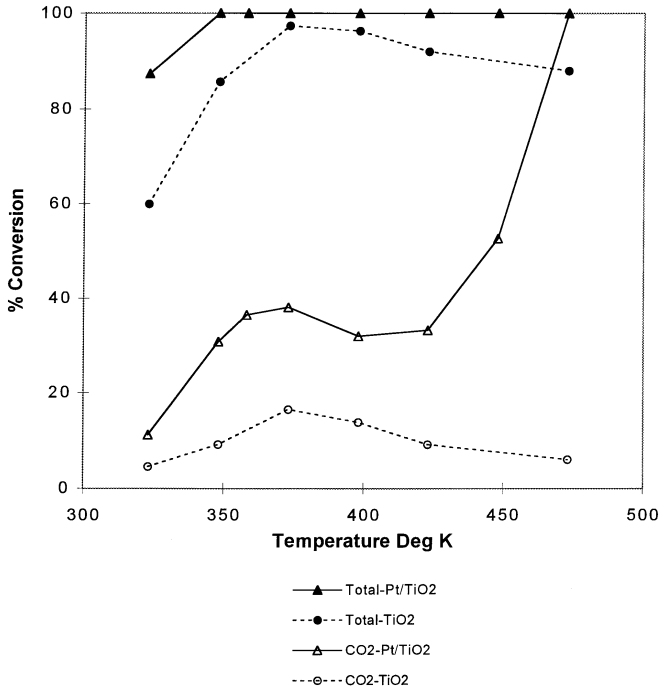

FIG. 3. Comparison of photo-reduced Pt/TiO_2 (PD Pt/TiO_2 0.2 wt%) and TiO_2. Shows percentage of total conversion of ethanol (% acetaldehyde + % CO_2) and percentage of conversion to CO_2 under illuminated standard reaction conditions; 7 mg catalyst, 6400 ppm ethanol, 20% oxygen, 30 sccm. TiO_2 is inactive in the dark up to about 473 K.

were conducted with TiO_2 that was deposited via an aqueous suspension, never heated beyond the reaction temperatures, and is, therefore, extensively hydroxylated.

Several studies have been conducted concerning the kinetics and intermediates of ethanol photo-oxidation over TiO_2 at ambient temperatures (33, 34, 39). Sauer *et al.* (33) first proposed the existence of a series-parallel oxidation pathway for ethanol to CO_2. They proposed that ethanol could be oxidized in series through the intermediate acetaldehyde to CO_2 (ethanol $\rightarrow$ acetaldehyde $\rightarrow$ CO_2) or by a parallel route through the formaldehyde intermediate (ethanol $\rightarrow$ acetaldehyde $\rightarrow$ formaldehyde $\rightarrow$ CO_2). More recently, using isotopically labeled transient photocatalytic studies, coupled with temperature programmed desorption, Muggli *et al.* (34) have detected the presence of strongly adsorbed surface intermediates, acetic and formic acid. These authors also confirmed parallel pathways, one pathway through acetic acid (acetaldehyde $\rightarrow$ acetic acid $\rightarrow$ formaldehyde $\rightarrow$ formic acid $\rightarrow$ CO_2), the other through formaldehyde (acetaldehyde $\rightarrow$ formaldehyde $\rightarrow$ formic acid $\rightarrow$ CO_2).

Nimlos *et al.* (39) in transient batch reactor studies suggested that acetaldehyde oxidation was the rate limiting step. Dark adsorption isotherms were measured, indicating that the adsorption equilibrium constant for acetaldehyde was about a factor of five smaller than that for ethanol. Muggli *et al.* (34), however, determined that adsorbed acetaldehyde was strongly adsorbed and decreased the activity of other intermediates. In addition, they determined that the (ethanol $\rightarrow$ acetaldehyde) and the (formaldehyde $\rightarrow$ formic acid $\rightarrow$ CO_2) steps proceed relatively quickly and are not rate limiting.

Our results, carried out at steady state and high concentrations of ethanol, show the presence of acetaldehyde in the gas phase, indicating that acetaldehyde must desorb from the TiO_2 surface, rather than being completely oxidized to CO_2. The observed increase in both the acetaldehyde and CO_2 production upon increasing the temperature to 373 K demonstrates that a thermally activated process other than the photo-reaction is causing the increase in reaction rates. Although not shown, the same trend in conversions shown in Figure 3 is seen at even higher ethanol concentrations of 38,500 ppm where the total conversion was only 20%. On the other hand, at lower ethanol concentrations of 2500 ppm, where the total conversion was 100% at 323 K, CO_2 conversion increased sharply to 100% by 373 K. Therefore, we propose that desorption of water as well as ethanol from the surface must free up sites necessary for the photo-oxidation of ethanol. Water is at least as strongly adsorbed as ethanol (32) and can displace adsorbed acetaldehyde (34). It therefore seems probable that desorption of water as well as ethanol facilitates the subsequent reactions of ethanol (to acetaldehyde and to CO_2), leading to increased photoactivity, which peaks at 373 K. A reaction following Langmuir–Hinshelwood kinetics and requiring an adjacent vacant site would show such a maximum in reaction rate with increasing temperature.

Photocatalytic Oxidation of Ethanol over Pt/TiO_2

Studies were conducted with the goal of defining the contours of oxidation rates seen when light and heat was applied to Pt/TiO_2. Photocatalysts prepared by photoreduction were used for these studies. After having observed a distinct photothermal synergism, we first examined the possible role of a Schottky barrier/electron trapping mechanism. Next, the role of catalyst preparation and weight loading was explored. Acidic etching of TiO_2 by chloroplatinic acid was implicated in reduced photoactivities. To test this hypothesis, TiO_2 layers were added sequentially to the Pt/TiO_2 to determine whether the addition of unetched TiO_2 would increase activities. These experiments are described below.

Synergistic effects. Oxidation of ethanol over Pt/TiO_2 under photothermal conditions displays distinct variations over the temperature range of 323 to 473 K. Figure 3 shows the photoactivity under photothermal conditions for photoreduced Pt/TiO_2 (0.2 wt%) versus TiO_2. Both total conversion and conversion to CO_2 are shown. CO_2 and acetaldehyde are the major products with a maximum of about 1.5% formaldehyde under illuminated conditions. No

formaldehyde was detected as a product in ethanol oxidation over Pt under dark conditions. Three regimes are present in conversion to CO_2 over the photoreduced catalysts. The first regime is from 323 to 373 K, where the photo-contribution from TiO_2 dominates and the thermal activity for CO_2 production over Pt is minimal. As previously discussed, it is likely that over this temperature range, desorption of water (and ethanol) from TiO_2 serves to free active sites, causing an increase in both acetaldehyde production and CO_2 production. Over the second regime, from 373 to 423 K, the conversion to CO_2 is decreasing. It is probable that, at these temperatures, the decrease in conversion to CO_2 over Pt/TiO_2 is caused by the dominating influence of lower steady state coverages of ethanol and acetaldehyde over TiO_2, the same processes we have previously attributed to decreasing CO_2 conversions over TiO_2. Finally, over the temperature range from 423 to 473 K, the conversion to CO_2 is increasing exponentially, similar to the thermal CO_2 production over Pt, which has become significant at this temperature, implying the enhanced CO_2 production under illuminated conditions is occurring over Pt.

Figure 4 shows the dark reaction versus the illuminated reaction. Again, although not shown, under dark conditions TiO_2 has no activity for ethanol oxidation up to about 473 K. Although the dark activity for acetaldehyde oxidation over TiO_2 was not tested, decreasing CO_2 conversions over illuminated TiO_2 at higher temperatures, as shown in Fig. 3, indicate that acetaldehyde oxidation is not thermally activated over TiO_2 at these temperatures. The dark reaction shown in Fig. 4 up to 500 K is due to thermal reaction over Pt. The illuminated Pt/TiO_2 achieves the same selectivity to CO_2 at temperatures that are lower by 150 K, compared to the dark reaction over Pt. In Fig. 5, the CO_2 production for illuminated TiO_2, Pt/TiO_2, and unilluminated Pt/TiO_2 is replotted for comparison. It is seen that the activity for CO_2 production over the illuminated Pt/TiO_2 is much greater than the sum of the illuminated TiO_2 and dark Pt/TiO_2. The net increase in conversion to CO_2 (illuminated Pt/TiO_2 − dark Pt/TiO_2 − illuminated TiO_2) is about 70% at 473 K. The enhanced CO_2 production under illuminated conditions becomes more apparent at higher temperatures (>373 K), where the total conversion of ethanol has taken place and the dark activity for CO_2 production over Pt has become significant. As previously shown, the production of acetaldehyde over TiO_2 remains about constant above 373 K; therefore the large increase in CO_2 production over illuminated Pt/TiO_2 at higher temperatures (>373 K) may be primarily related to thermal oxidation over Pt of acetaldehyde, photo-produced over TiO_2. While this is a plausible explanation where 100% conversion of ethanol has occurred and Pt is thermally active, the results are harder to explain at 323 K, where total conversion is less than 100%, and Pt thermal activity is minimal. Here, the Pt/TiO_2 shows an increase in both CO_2 production and total conversion, compared to the TiO_2. It is possible that a contribution due to a Schottky barrier electronic effect is responsible for the increased conversions at this temperature.

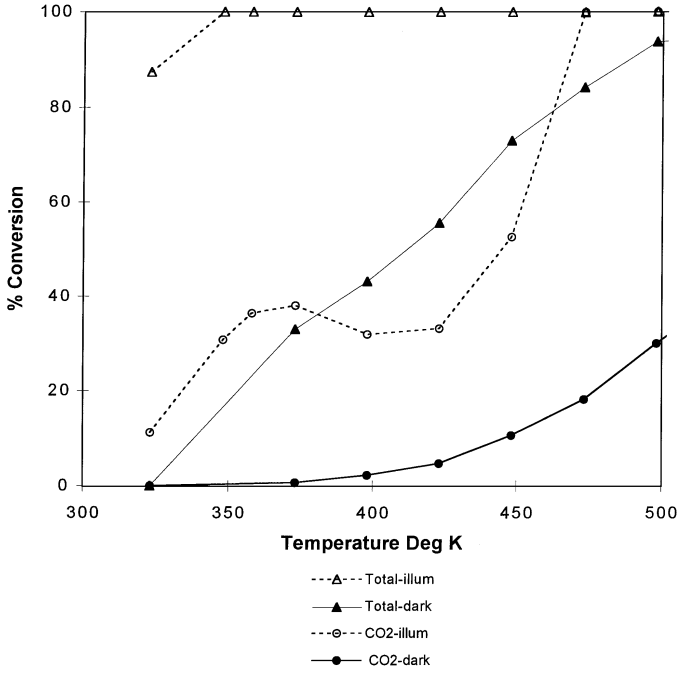

FIG. 4. Comparison of photo-reduced Pt/TiO_2 (0.2 wt%) under illuminated and dark conditions at standard reaction conditions. Dark activity is attributable to Pt.

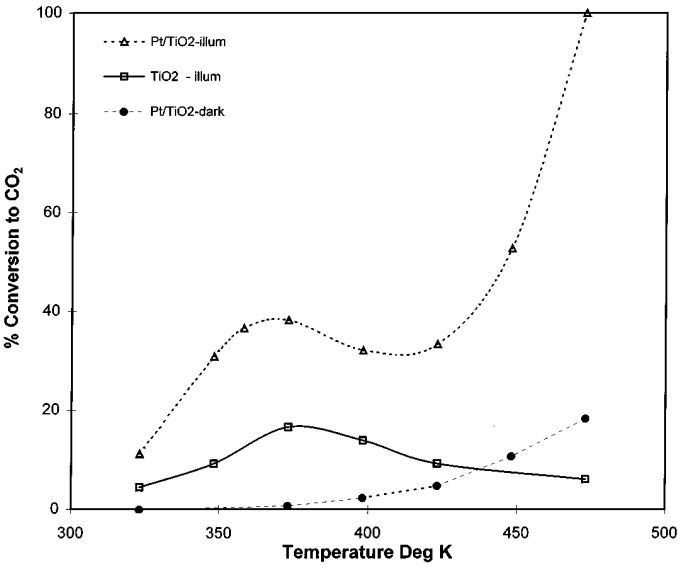

FIG. 5. Percentage of CO_2 conversion in Figs. 3 and 4 replotted for comparison of photo-reduced Pt/TiO_2 under illuminated and dark conditions compared to TiO_2 under illuminated conditions. Synergism for conversion to CO_2 is revealed where illuminated Pt/TiO_2 activity is greater than the sum of illuminated TiO_2 and dark Pt/TiO_2 activity.

Physical Mixture of Pt/SiO_2 and TiO_2

A process that has been thought (11, 14–18) to aid photocatalytic activity in liquid phase studies of Pt/TiO_2 is improved charge separation caused by electron trapping by Pt or as a result of a Schottky barrier at the Pt–TiO_2 interface. Electron trapping may increase rates of electron transfer to acceptors (oxygen) on the Pt surface, increasing O^- or O_2^- species, which may participate in electrophilic or nucleophilic attack on neighboring, adsorbed organics. Alternatively, improved charge separation may aid oxidation efficiencies by increasing hole lifetimes in the TiO_2 by lowering electron–hole recombination rates. In order to test for the presence of electronic effects related to Pt supported on TiO_2, we examined the photoactivity of a physical mixture of Pt/SiO_2 and TiO_2, described below.

We reasoned that Pt supported on silica, but in close proximity with TiO_2, would not be as effective as Pt supported on TiO_2 if electronic effects were the cause of the synergism. Silica is not a photocatalyst and has no thermal activity for oxidation of ethanol at the temperatures investigated. Therefore, any beneficial effect on the photoactivity of a physical mixture of Pt/SiO_2 and TiO_2 must arise from the separate effects of the thermal activity of the Pt and the photoactivity of the TiO_2. The dark and illuminated activity of a 50/50 wt% mixture of Pt/SiO_2 and TiO_2 was examined for evidence of photothermal synergism. The total weight of catalyst was 7 mg and had an overall 0.2 wt% loading of Pt based on the total weight of TiO_2 and SiO_2. The amount of TiO_2 in the reactor was half the amount present in the case of the 0.2 wt% Pt/TiO_2 catalyst shown in Fig. 4.

The illuminated versus dark activity, shown in Fig. 6, reveals that CO_2 production is enhanced under illuminated conditions, especially at temperatures greater than 373 K. The enhancement, however, is not as pronounced as in the case of the photoreduced catalyst shown in Fig. 4. Both total conversion and conversion to CO_2 are substantially lower under illuminated conditions on the Pt/SiO_2 physical mixture, compared to the photoreduced 0.2 wt% Pt/TiO_2 catalyst. This may be partly explained by the fact that half the amount of TiO_2 is present in the physical mixture, compared to the photoreduced catalyst. The similar dark activity for both the catalysts indicates that they have a similar amount of Pt available for reaction. Above about 373 K, the conversion to CO_2 is again greater than the sum of that expected from the illuminated TiO_2 and dark Pt/TiO_2. The presence of a similar synergistic effect with half the amount of TiO_2, but the same amount of Pt, indicates that the photoactivity of the TiO_2 is important to the enhancement of CO_2 production over Pt/TiO_2 under illuminated conditions. Since a Pt–TiO_2 interface is not present, we conclude that electronic effects do not contribute substantially to the observed synergistic increase in CO_2 production, at least above 373 K. The major contribution to the synergism appears to be gas phase transport of acetaldehyde, produced by photo-oxidation of ethanol over TiO_2, to Pt where thermal oxidation to CO_2 takes place.

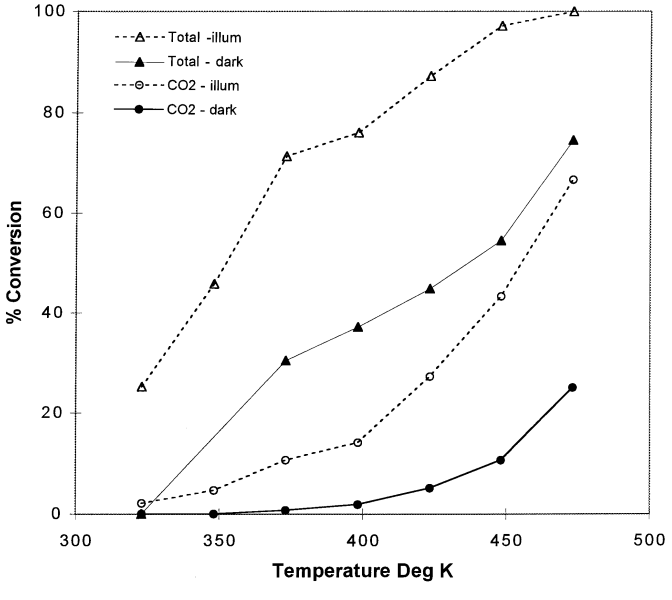

FIG. 6. Comparison of illuminated and dark activity of a physical mixture 50/50 wt% Pt/SiO_2-TiO_2 with an overall Pt weight loading of 0.2 wt%.

Effect of Ethanol Concentration on Photo-Reduced Catalysts

Figure 7 shows the effect of ethanol concentration on the activity of the photo-reduced Pt/TiO_2 (0.2 wt%) catalyst at 373 K. At ethanol concentrations lower than 7700 ppm under illuminated conditions, 100% conversion efficiency to CO_2 is achieved. At higher ethanol concentrations, the conversion to CO_2 under photothermal conditions drops off quickly. The conversion to CO_2 over Pt (dark conditions) is less than 1% at 373 K over the entire concentration range. Although not shown, 100% conversion to CO_2 is achieved at 323 K for ethanol concentrations lower than about 2560 ppm. At 323 K, the dark activity of Pt is insignificant, and the entire activity is attributable to illuminated Pt/TiO_2.

A quantum yield for photo-oxidation of ethanol over TiO_2 may be estimated by using the ethanol concentration where 100% conversion to CO_2 is achieved at 323 K. Since stoichiometric conversion is achieved as shown in [1] and assuming a 12 electron-hole oxidation process for each mole of ethanol oxidized to CO_2, one may calculate a quantum yield based on (six times moles of CO_2 produced/moles of light adsorbed). Using a light intensity at 356 nm of 2.4×10^{-8} Ein/s-cm^2 and a measured adsorption coefficient 4.2 cm^2/g at 356 nm, the quantum yield is estimated to be between 7.7 and 11.6%. This can be compared with other researchers (38) who found quantum yields of 18% for photodegradation of gaseous acetaldehyde (a 10 electron–hole oxidation) over P25 an initial concentrations of 2400 ppm.

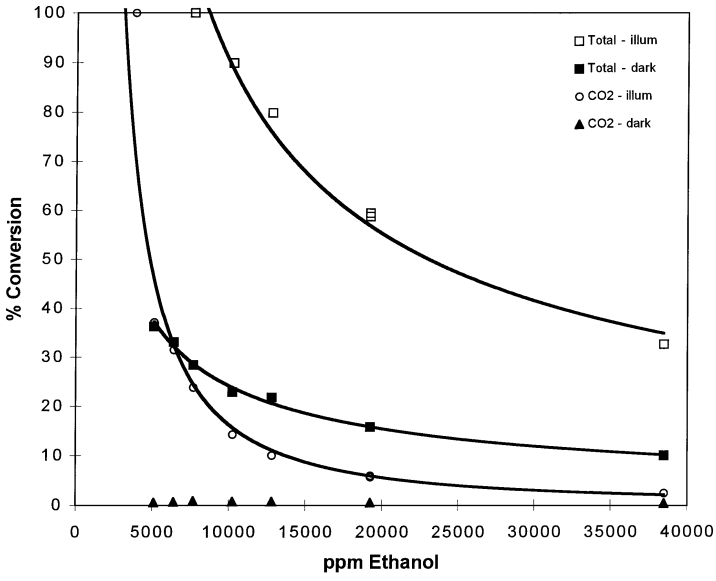

FIG. 7. Comparison of illuminated and dark activity of photo-reduced Pt/TiO_2 (0.2 wt%) at 373 K with varying ethanol concentration.

Determining quantum yields at higher temperatures is not meaningful since thermal activity from Pt contributes and it is difficult to separate the photo and thermal contributions to the total activity.

The suppressed conversion to CO_2 over TiO_2 as the ethanol concentration is increased may be attributed to competitive adsorption of ethanol, excluding re-adsorption of acetaldehyde. The equilibrium adsorption constant of acetaldehyde over TiO_2 has been found to be approximately five times less than that of ethanol (39). In addition, the rate limiting step for complete oxidation is not the oxidation of ethanol to acetaldehyde (34), but more likely the re-adsorption and subsequent oxidation of acetaldehyde. Therefore, the strong competition of ethanol for reaction sites would be expected to lower CO_2 production.

Effect of Pt Weight Loading on Photo-Reduced Catalysts

The effect of weight loading was of interest since previous researchers (41, 42) had indicated that there was an ideal weight loading of Pt (1.0 wt%) for photo-oxidation of liquid phase alcohols. Since the Pt particles were the same diameter (2 nm) over a range of weight loadings, these researchers suggested that a 1.0 wt% loading provided an optimal distribution of charge carriers within the photocatalyst at a certain Pt particle coverage. On the other hand, UHV studies by Linsebigler *et al.* (43) showed that increasing Pt coverage decreased photo yields of CO_2 from illuminated oxidation of co-adsorbed CO and O_2 at 105 K. It was reasoned that Pt deposited by vapor deposition on TiO_2 rutile (110) nucleated at oxygen vacancy sites, which had been found to be active photocatalytic sites, thereby blocking the number of available photoactive TiO_2 sites. These researchers did not have TEM images but estimated the Pt cluster size to be 1.6 nm with a spacing of 2.8 nm between cluster centers. This can be compared with our photocatalysts showing about a 2-nm Pt particle size with a distance on the order of 4–7 nm between particles.

Ethanol oxidations were carried out with two different weight loadings of Pt on photo-reduced Pt/TiO_2 (0.2 and 0.4 wt%). The Pt particles for the 0.2 wt% sample were unresolvable by HRTEM (<1 nm) and are considered to have a dispersion of 100%. The 0.4 wt% sample has 2-nm diameter Pt particles, corresponding to a dispersion of about 77%. Figure 8 shows a comparison of conversions under

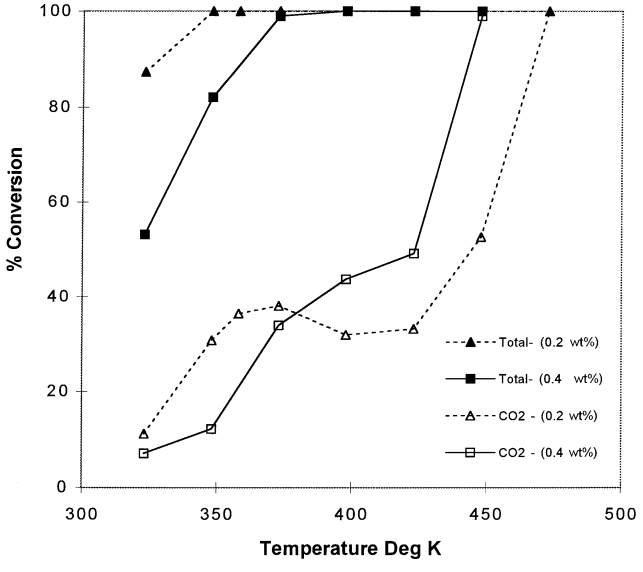

FIG. 8. Comparison of activities under illuminated standard reaction conditions of photo-reduced Pt/TiO_2 at 0.2 wt% and 0.4 wt% Pt weight loading.

illuminated conditions as a function of temperature for the two Pt weight loadings. At low temperatures, where TiO_2 activity dominates, the higher Pt weight loading catalyst shows decreased activity. Conversely, this catalyst shows higher activity at higher temperature where Pt activity dominates. Since the fractional coverage of the TiO_2 surface by Pt at 0.4 wt% loading is estimated at about 1.5%, it does not seem likely that the decrease in activity at lower temperatures is caused by Pt blocking TiO_2 photo-active sites. If Pt nucleating at photo-active sites was a substantial factor, the Pt/TiO_2 catalyst with half the Pt weight loading, but smaller Pt particles, would have a similar number of Pt-nucleated TiO_2 sites and would be expected to show a similar decrease in activity at lower temperatures. It is more likely that changes to the TiO_2 surface caused by slight acidic etching, previously pointed out in Fig. 2b, has affected the photoactivity of TiO_2. The increase in CO_2 conversion at higher temperatures, where Pt activity dominates, can be explained by the higher number of available Pt sites for reaction.

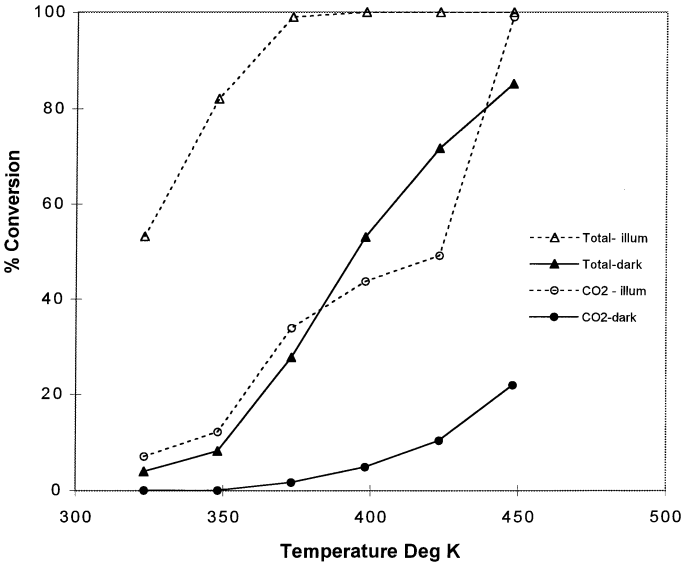

FIG. 9. Activity of photo-reduced catalyst (PD Pt/TiO_2, 0.4 wt%) under illuminated and dark standard reaction conditions.

Thermally Reduced vs Photo-Reduced Catalysts

The photoactivity of a thermally reduced Pt/TiO_2 catalyst (Pcl Pt/TiO_2, 0.4 wt%) was compared to the photo-reduced catalyst to study the effects of catalyst preparation. The thermally reduced catalyst was prepared by adsorption of the $PtCl_6^-$ anion at about pH 2.00. Compared to the photoreduced catalyst, it exhibited a higher degree of acidic etching of the TiO_2 surface with the formation of an amorphous layer as shown in Fig. 2c. It is believed that the higher degree of acidic etching for the thermally reduced catalyst could be related to the fact that it is not washed after adsorption of $PtCl_6^-$ anion and is in contact with the unreduced anionic solution for a longer period. Pt weight loadings for both the photo-reduced and thermally reduced catalyst are about the same (0.4 wt%) and have similar Pt particle sizes, 2 and 1.3 nm, respectively.

Figure 9 shows the total conversion and conversion to CO_2 under illuminated and dark conditions for the photoreduced Pt/TiO_2 (0.4 wt% Pt). Figure 10 shows the corresponding data for a thermally reduced catalyst at the same weight loading. The total conversion is significantly lower for the thermally reduced catalyst compared to the photoreduced catalysts under illuminated conditions, while the dark conversions are similar. Although not shown, tests on other thermally reduced catalysts with etched TiO_2 surfaces showed a similar detrimental effect on total conversions under illuminated conditions. Specifically, much less acetaldehyde, the primary product of photo-oxidation over TiO_2, is being produced over the thermally reduced catalyst. The Pt/SiO_2-TiO_2 physical mixture with half the amount of TiO_2 but the same amount of Pt shows a similar synergistic effect compared to the thermally reduced Pt/TiO_2 with an etched TiO_2 surface. This suggests that photo-oxidative production of acetaldehyde over TiO_2 is necessary for the synergistic effect that leads to increased CO_2 production over Pt under illuminated conditions.

We have previously shown that a higher weight loading of photo-reduced Pt reduces total conversions at lower temperatures. A close inspection of the HRTEM micrographs of the both the photoreduced and thermally reduced catalysts, Figures 2a–c, shows a corresponding trend of increased surface roughness of the TiO_2 with formation of an amorphous TiO_2 layer on the thermally reduced catalyst from acidic etching. Shah *et al.* (44) have recently

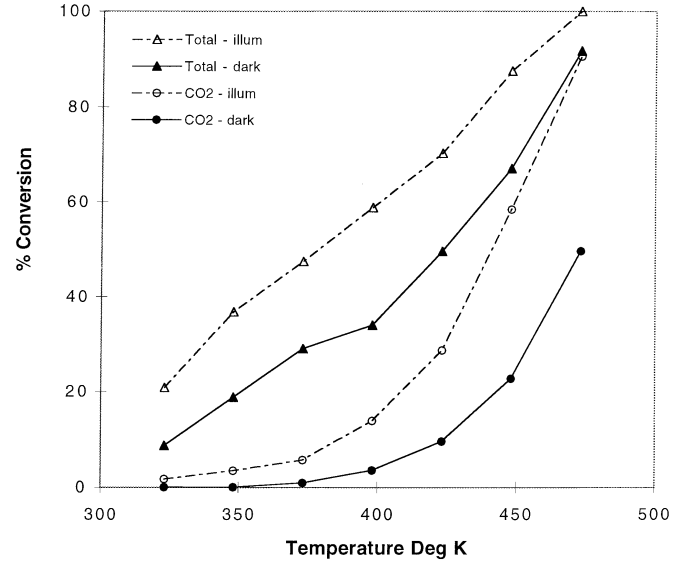

FIG. 10. Activity of thermally reduced catalyst (Pcl Pt/TiO_2, 0.4 wt%) under illuminated and dark standard reaction conditions.

investigated the effect of ionic strength and pH on the adsorption of Pt complexes on alumina and silica. Although the effect of oxide dissolution at low and high pH in retarding metal adsorption was discussed, an additional important effect of oxide dissolution on metal loaded catalysts is the changed nature of the oxide surface caused by oxide dissolution, especially if it contributes to catalytic mechanisms. Conversely, the absence of a synergistic effect at temperatures lower that 373 K by the Pt/SiO_2–TiO_2 physical mixture and the thermally reduced catalysts demonstrates the absence of electronic effects compared to the photo-reduced catalysts.

The presence or absence of reduced bulk TiO_2 may be an important consideration. Torimoto *et al.* (45) and Chen *et al.* (29) have reported the formation of bluish colored powder TiO_2 created by high intensity laser radiation and high temperature reduction in H_2. The light bluish colored TiO_2 is stable in air and has been attributed to the formation of bulk Ti^{3+}, seen in ESR studies but not in XPS studies. Chen *et al.* (29) and Belton *et al.* (46) have suggested that the presence of bulk reduced TiO_2 is necessary for SMSI attributable to Schottky barrier formation at the Pt/TiO_2 interface. Our photo-reduced Pt/TiO_2 samples also exhibited a light blue color, which was stable in air and showed evidence of SMSI as reflected by reduced H_2 uptake, previously discussed. Bulk reduction in our catalyst could have been caused during the photodeposition process. This difference might explain the presence of increased conversions seen with the photo-reduced Pt/TiO_2 at <373 K, where Pt thermal activity is minimal and its absence in the thermally reduced catalysts which showed no evidence of bulk reduced TiO_2.

Layered Bed Experiment

To further investigate whether the reduced photoactivity for the thermally reduced Pt/TiO_2 was related to the loss of photoactivity caused by the etching of TiO_2, additional TiO_2 was added to the thermally reduced Pt/TiO_2 particulate film, and the photoactivity examined. We chose this method since we were not able to produce a suitably etched TiO_2 sample by treating the TiO_2 with HCl, suggesting that the dissolution may not be simply related to the pH.

A thin film of Pt/TiO_2 (7.4 mg) was deposited in the manner previously described and the activity measured. Additional TiO_2 was then evenly deposited sequentially in total amounts of 3.9, 3.7 and 7.3 mg as shown in the schematic in Fig. 11. The fraction of incident light transmitted was calculated from an absorption coefficient derived as described earlier. As shown in Fig. 11, all the catalyst layers are illuminated in this arrangement. Although not shown, the thermally activated dark activity over Pt remains essentially unchanged by addition of TiO_2. This indicates a lack of mass transport limitations in gas phase transport of organics and oxygen to the Pt in the bottom layer of catalyst.

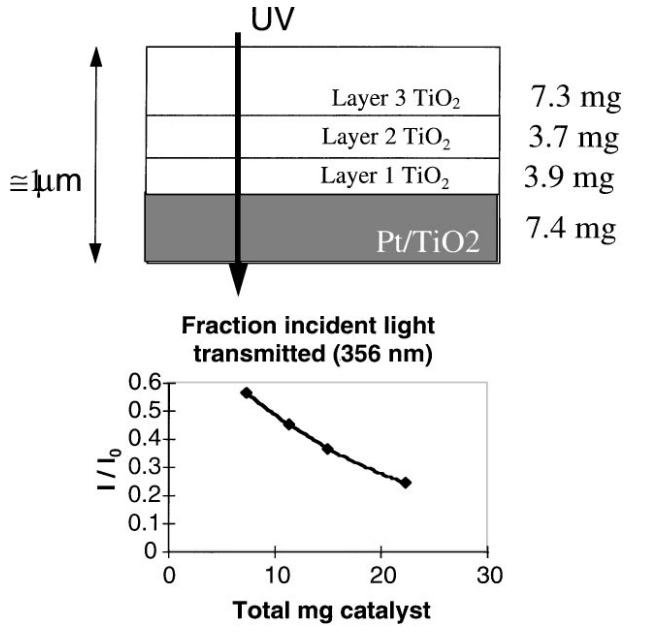

FIG. 11. Experimental schematic of layered bed experiment where illuminated and dark activities are determined sequentially after addition of TiO_2 to thermally reduced Pt/TiO_2 (Pcl Pt/TiO_2, 0.4 wt%). The fraction of incident light intensity transmitted through the particulate film after addition of each layer, calculated from a known absorption coefficient, is shown.

Figure 12 shows that under illumination, addition of TiO_2 consistently increases the total conversion, mostly through acetaldehyde production, as would be expected. Figure 13 shows CO_2 production is increased by addition of the first layer of TiO_2; remains about the same after addition of the

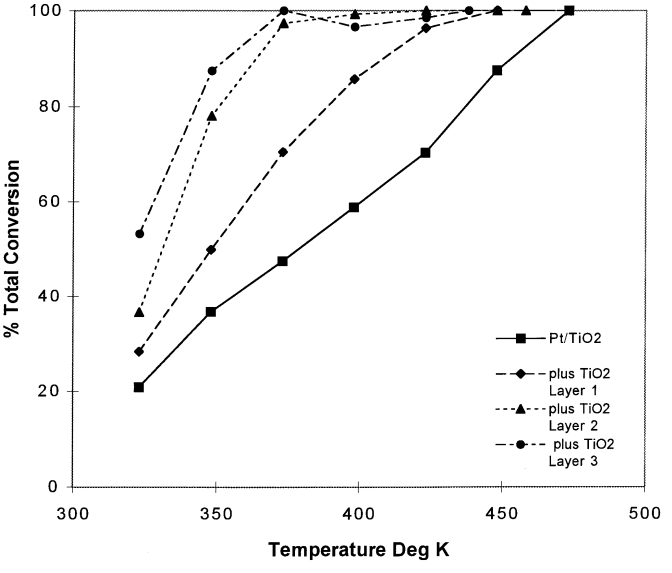

FIG. 12. Percentage of total conversion under illuminated conditions is shown for the thermally reduced Pt/TiO_2 at 0.4 wt% Pt loading, determined sequentially after addition of TiO_2 layers on top of the Pt/TiO_2.

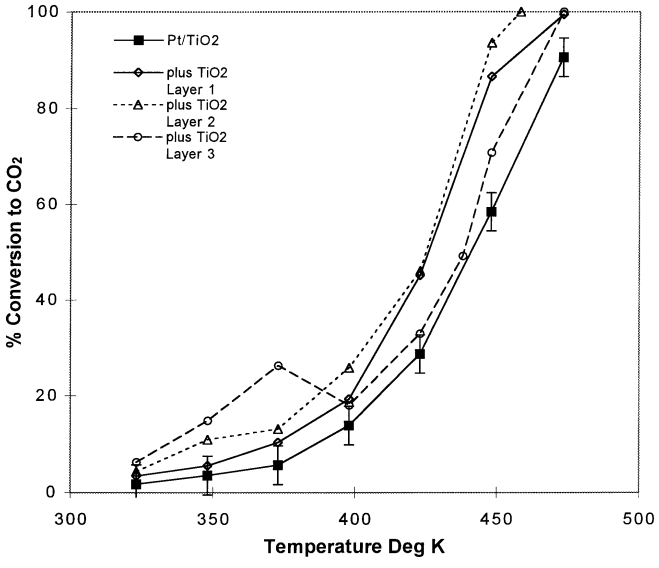

FIG. 13. Percentage of conversion to CO_2 under illuminated conditions is shown for the thermally reduced Pt/TiO_2 at 0.4 wt% Pt loading, determined sequentially after addition of TiO_2 layers on top of the Pt/TiO_2.

second layer; and decreases at higher temperatures after addition of the third layer of TiO_2. At lower temperatures (<373 K) the conversion to CO_2 increases with added TiO_2, but the conversion can be attributed to TiO_2 alone, with the absence of any apparent synergistic effect at these temperatures. In an effort to better quantify the effect of the synergy, we have shown in Fig. 14 the CO_2 selectivity under illumination after subtracting the dark selectivity. The selectivities represent the experimentally observed increase in CO_2 production due to illumination. The selectivity increase due to illumination, alone, is plotted versus an effective weight percentage Pt calculated by including the added TiO_2. A maximum increase in selectivity for complete oxidation is seen for temperatures greater than 373 K at about an overall weight loading of 0.25 wt% Pt. At higher temperatures, there appears to be an ideal Pt/TiO_2 ratio for enhanced CO_2 production over Pt that is related to gas phase transport of photo-produced acetaldehyde. The synergistic effect increases at higher temperatures as acetaldehyde is more quickly oxidized to CO_2 over Pt. Since the second and third added TiO_2 layers reach 100% total conversion at lower temperature than the first added layer, yet show decreased CO_2 selectivity, increases in selectivity are not merely related to more acetaldehyde being available for reaction at higher temperatures. It is believed that decreases in CO_2 selectivity as additional TiO_2 is added are caused by competitive adsorption of acetaldehyde to the exclusion of O_2 over the Pt.

These results indicate that addition of TiO_2 can increase selectivity to CO_2 under illuminated conditions. By adding TiO_2 to a thermally reduced Pt/TiO_2 catalyst (which shows acidic etching of TiO_2) CO_2 production at temperatures greater than 373 K becomes similar to that of a photoreduced Pt/TiO_2. Pt/TiO_2 catalysts with a progressively etched TiO_2 surface show reduced photoactivity as seen in much lower acetaldehyde production over TiO_2 and conversion to CO_2 over Pt. Gas phase transport to Pt of partial oxidation products produced over TiO_2 appears to be important for increases in complete oxidation efficiencies at temperatures greater than 373 K. Maximizing the synergistic oxidation of ethanol to CO_2 over TiO_2 and Pt will require a better knowledge of complicated competitive adsorption

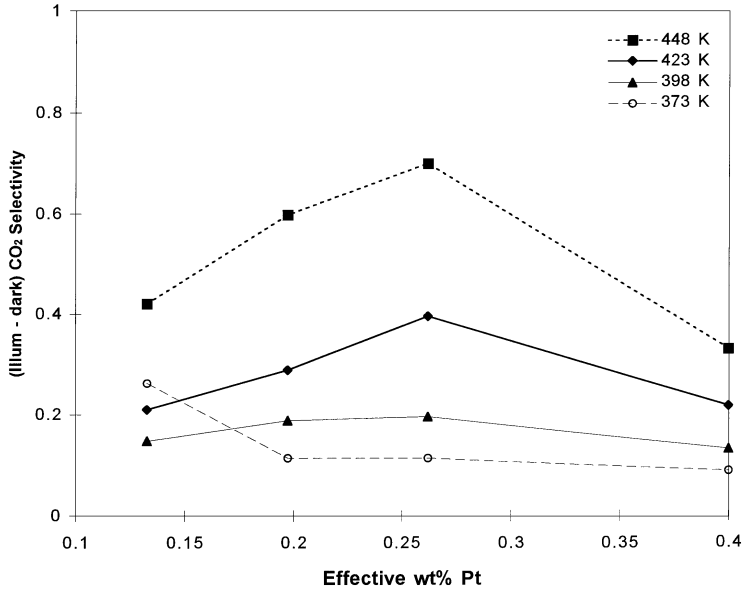

FIG. 14. Illuminated minus dark CO_2 selectivity is shown at selected temperatures for the layered bed where the wt% Pt is calculated by including the TiO_2 in the total catalyst weight.

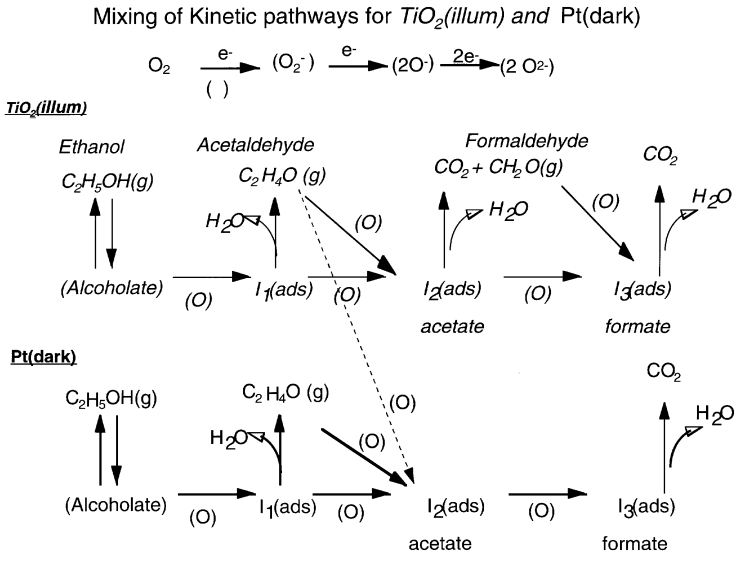

FIG. 15. Schematic of major kinetic pathways for ethanol oxidation over photoactivated TiO_2 and thermally activated Pt. Dotted arrow indicates transport of the photo-oxidized intermediate, acetaldehyde, produced over TiO_2, to the Pt where it is thermally oxidized to CO_2.

effects where both reactant concentrations and Pt weight loadings are important.

Nature of Photothermal Synergism

Figure 15 shows kinetic pathways that are similar for ethanol oxidation over Pt and TiO_2. The schemes are not intended to reflect elementary steps and therefore say nothing about mechanisms; however, they allow the observed kinetics to be explained schematically. These schemes are generally consistent with reported results on thermal oxidation of ethanol over Pt and photo-oxidation over TiO_2. Previous studies of ethanol oxidation over Pt (47, 48) have proposed a series-parallel oxidation route similar to ethanol oxidation pathways over TiO_2 proposed by Sauer *et al.* (33) and Muggli *et al.* (34).

Gonzalez and Nagal (49, 50) studied the oxidation of acetaldehyde and ethanol over Pt/SiO_2 catalysts. They determined that the oxidation of acetaldehyde proceeds by a Langmuir–Hinshelwood mechanism where the rate determining step is reaction between surface oxygen and adsorbed acetaldehyde species. Using IR spectroscopy, they identified an acetate surface species formed from an adsorbed ethoxy that was subsequently oxidized to CO_2. They suggested that a direct series oxidation pathway to CO_2, involving only surface intermediates, prevailed over Pt at higher temperatures. Our results, at higher ethanol concentrations, suggest that gaseous acetaldehyde is produced primarily via photo-oxidation of ethanol over TiO_2, with acetaldehyde production constant over the temperature range 373 K to 473 K. At temperatures greater than 373 K, where Pt thermal activity for acetaldehyde oxidation becomes significant, the oxidation pathway to CO_2 over Pt/TiO_2 favors the route through gaseous acetaldehyde.

Figure 15 depicts a mixed series-parallel scheme for ethanol oxidation over Pt and illuminated TiO_2. An increase in the concentration of the partial oxidation product, acetaldehyde, produced over illuminated TiO_2 will increase the rate of CO_2 production over Pt. This explains why adding TiO_2 to the etched Pt/TiO_2 increases conversions to CO_2 above 373 K, where Pt activity from thermal oxidation dominates. Since the photo-production of acetaldehyde over TiO_2 is constant above about 373 K, addition of TiO_2 provides a constant source of acetaldehyde for re-adsorption and conversion to CO_2 over Pt. The higher concentration of acetaldehyde produced by photoactivation over TiO_2 can explain the increased CO_2 production seen under illuminated conditions for Pt/TiO_2 at temperatures greater than 373 K.

CONCLUSIONS

An improved photocatalyst was made by coupling a good thermal oxidation catalyst, Pt, with a good partial oxidation photocatalyst, TiO_2, by supporting nanometer size particles of Pt on TiO_2. Simultaneous photo and thermal activation of the Pt/TiO_2 photocatalyst resulted in unique synergistic effects at moderate temperatures (<473 K). Complete oxidation activity was greater than that of photoactivity of TiO_2 plus the thermal activity of Pt for all catalysts at temperatures greater than 373 K. Some evidence of an electronic effect was seen at temperatures lower than 373 K, where the thermal activity of Pt is minimal. This low temperature effect was absent for thermally reduced catalysts and Pt/SiO_2-TiO_2 physical mixtures. It is speculated that bulk reduced TiO_2 is formed during the photodeposition procedure and could be related to an electronic effect

that is most apparent at low temperatures where the thermal activity of Pt is minimal. A different synergistic effect present at temperatures greater that 373 K is attributed to interaction of similar mixed series-parallel reaction pathways occurring thermally over Pt and photoactively over TiO_2. At temperatures greater than 373 K, the synergistic effect was seen for all catalysts but was larger for the photo-reduced Pt/TiO_2. Progressive acidic etching of the TiO_2 surface by chloroplatinic acid can decrease photothermal activities over all temperature ranges for catalysts at similar weight loadings and Pt dispersions. Photo-oxidative production of acetaldehyde is decreased over etched TiO_2 surfaces, lowering selectivities for CO_2 production over Pt. Increasing acidities of chloroplatinic acid solutions to achieve higher Pt weight loadings can increase acidic etching of TiO_2. The largest synergistic effects are seen at low temperature for the lowest weight loadings of photo-reduced Pt/TiO_2, where Pt particles are not resolvable by HRTEM. At higher temperatures, thermally reduced Pt/TiO_2 with unetched TiO_2 added has an optimal synergism at similarly low (0.2–0.3 wt%) loadings of Pt. Further studies are needed to better define the conditions for achieving an optimal synergistic effect, however, it appears that competitive adsorption effects over both TiO_2 and Pt may play important roles.

ACKNOWLEDGMENTS

This research was supported by NSF Grant HRD 93-53208 and by the Waste Management Education and Research Consortium (WERC) of New Mexico.

REFERENCES

1. Fujishima, A., and Honda, K., *Nature* **37**, 238 (1972).
2. Turchi, C. S., and Ollis, D. F., *J. Catal.* **122**, 178 (1990).
3. Pelizzetti, E., and Minero, C., *Electrochim. Acta* **38**, 47 (1993).
4. Draper, R. B., and Fox, M. A., *Langmuir* **6**, 1396 (1990).
5. Djeghri, N., and Teichner, S. J., *J. Catal.* **62**, 99 (1980).
6. Bickley, R. I., Munuera, G., and Stone, F. S., *J. Catal.* **31**, 398 (1973).
7. Cunningham, J., and Hodnett, B., *J. Chem. Soc., Faraday Trans. 1* **77**, 2777 (1981).
8. Liu, Y. C., Griffin, G. L., Chan, S. S., and Wachs, I. E., *J. Catal.* **94**, 108 (1985).
9. Lu, G., Linsebigler, A., and Yates, J. T., Jr., *J. Phys. Chem.* **99**, 7626 (1995).
10. Wong, J. C. S., Linsebigler, A., Lu, G., Fan, J., and Yates, J. T., Jr., *J. Phys. Chem.* **99**, 335 (1995).
11. Krauetler, B., and Bard, A. J., *J. Am. Chem. Soc.* **100**, 4317 (1978).
12. Pichat, P., Herrmann, J.-M., Disdier, J., Coubon, H., and Mozzanega, M.-N., *Nouv. J. Chim.* **5**, 627 (1981).
13. Ishitani, O., Inoue, C., Suzuki, Y., and Ibusuki, T., *J. Photochem, Photobiol. A: Chem.* **72**, 269 (1993).
14. Bard, A. J., *J. Photochem.* **10**, 59 (1975).
15. Disidier, J., Herrmann, J.-M., and Pichat, P., *J. Chem. Soc. Faraday Trans. 1* **79**, 651 (1983).
16. Schindler, K-M., and Kunst, M., *J. Phys. Chem.* **94**, 8222 (1990).
17. Wang, C-M., Heller, A., and Gerischer, H., *J. Am. Chem. Soc.* **114**, 5230 (1992).
18. Gersicher, H., *J. Phys. Chem.* **88**, 6096 (1984).
19. Fu, X. Z., Zeltner, W. A., and Anderson, M. A., *Appl. Catal. B-Env.* **6**, 209 (1995).
20. Lu, G., Linsebigler, A., and Yates, J. T., Jr., *J. Chem. Phys.* **102**, 4657 (1995).
21. Formenti, M., Juillet, F., Meriaudeau, P., and Teichner, S. J., *Chem. Tech.* **1**, 680 (1971).
22. Jacoby, W. A., Blake, D. M., Noble, R. D., and Koval, C. A., *J. Catal.* **157**, 87 (1995).
23. Reiss, R., Ryan, P. B., Tibbetts, S. J., and Koutrakis, P., *J. Air & Waste Manage. Assoc.* **45**, 811 (1995).
24. Jacoby, B., NREL, personal communication, re: radiometer measurements.
25. Messner, A. E., Rosie, D. M., and Argabright, P. A., *Anal. Chem.* **31**, 230 (1958).
26. Brunelle, P., *Pure Appl. Chem.* **50**, 1211 (1978).
27. Nargiello, M., and Herz, T., *in* "Photocatalytic Purification and Treatment of Water and Air" (D. F. Ollis and H. Al-Ekabi, Eds.), p. 169. Elsevier Science, Amsterdam, 1993.
28. Kennedy, J. C., III, "The Effects of TiO_2 Particulate Film Morphology and TiO_2 surface Characteristics on Photoactivity," Masters thesis, University of New Mexico, 1994.
29. Chen, B-H., and White, J. M., *J. Phys. Chem.* **86**, 3534 (1982).
30. Stöber, W., Fink, A., and Bohn, E., *J. Coll. Int. Sci.* **26**, 62 (1968).
31. Blake, N. R., and Griffin, G. L., *J. Phys. Chem.* **92**, 5697 (1988).
32. Lusvardi, V. S., Barteau, M. A., and Farneth, W. E., *J. Catal.* **153**, 41 (1995).
33. Sauer, M. L., and Ollis, D. F., *J. Catal.* **158**, 570 (1996).
34. Muggli, D. S., McCue, J. T., and Falconer, J. L., *J. Catal.*, submitted.
35. Muggli, D. S., Larson, S. A., and Falconer, J. L., *J. Phys. Chem.* **100**, 15886 (1996).
36. Sauer, M. L., and Ollis, D. F., *J. Catal.* **158**, 570 (1996).
37. Muggli, D. S., McCue, J. T., and Falconer, J. L., *J. Catal.*, submitted.
38. Sopyan, I., Watanabe, M., Murawawa, S., Hashimoto, K., and Fujishima, A., *J. Photochem. Photobio. A. Chem.* **98**, 79 (1996).
39. Nimlos, M. R., Wolfrum, E. J., Brewer, M. L., Fennell, J. A., and Binter, G., *Env. Sci. Tech.* **30**, 3102 (1996).
40. Peral, J., and Ollis, D. F., *J. Catal.* **136**, 554 (1992).
41. Herrmann, J.-M., Disdier, J., and Pichat, P., *in* "Metal-Support and Metal-Additive Effects in Catalysis" (B. Imelik *et al.*, Eds.), p. 27. Elsevier, Amsterdam, 1982.
42. Pichat, P., Mozzanega, M.-N., Disdier, J., and Herrmann, J.-M., *Nouv. J. Chim.* **11**, 559 (1982).
43. Linsebigler, A., Rusu, C., and Yates, J. T., Jr., *J. Am. Chem. Soc.* **118**, 5284 (1996).
44. Shah, A. M., and Regalbuto, J. R., *Langmuir* **10**, 500 (1994).
45. Torimoto, T., Fox, R. J., III, and Fox, M. A., *J. Eletrochem. Soc.* **143**, 3712 (1996).
46. Belton, D. N., Sun, Y.-M., and White, J. M., *J. Phys. Chem.* **88**, 1690 (1984).
47. McCabe, R. W., and Mitchell, P. J., *Ind. Eng. Chem. Prod. Res. Dev.* **22**, 212 (1983).
48. McCabe, R. W., and Mitchell, P. J., *Ind. Eng. Chem. Prod. Res. Dev.* **23**, 196 (1984).
49. Gonzalez, R. D., and Nagal, M., *Appl. Catal.* **18**, 57 (1985).
50. Nagal, M., and Gonzalez, R. D., *Ind. Eng. Chem. Prod. Res. Dev.* **24**, 525 (1985).